# Magnetic studies of magnetotactic bacteria by soft x-ray STXM and ptychography

Cite as: AIP Conference Proceedings **1696**, 020002 (2016); https://doi.org/10.1063/1.4937496
Published Online: 28 January 2016

X. H. Zhu, T. Tyliszczak, H.-W. Shiu, et al.



# Magnetic studies of magnetotactic bacteria by soft X-ray STXM and ptychography

X.H. Zhu,[1] T. Tyliszczak[2], H.-W. Shiu,[2,3] D. Shapiro,[2] D.A. Bazylinski[4], U. Lins[5] and A.P. Hitchcock[1,a]

[1]*Chemistry & Chemical Biology, McMaster University, Hamilton, ON, L8S 4M1, Canada*
[2] *Advanced Light Source, LBNL, Berkeley, CA, 94720, USA*
[3] *NSRRC, Hsinchu, 30076, Taiwan, R.O.C.*
[4] *Life Sciences, University of Nevada, Las Vegas, NV, 89154, USA*
[5]*Department de Microbiologia Geral, UFRJ, Rio de Janeiro, RJ, 2194-590, Brazil*

[a)] corresponding author: aph@mcmaster.ca

**Abstract.** Magnetotactic bacteria (MTB) biomineralize chains of nanoscale magnetite single crystals which align the cell with the earth's magnetic field and assist the cell to migrate to, and maintain its position at, the oxic-anoxic transition zone, their preferred habitat. Here we describe use of multi-edge scanning transmission X-ray microscopy (STXM) to investigate the chemistry and magnetism of MTB on an individual cell basis. We report measurements of the orientation of the magnetic vector of magnetosome chains relative to the location of the single flagellum in marine vibrio, *Magnetovibrio blakemorei* strain MV-1 cells from both the southern and northern hemisphere. We also report a major improvement in both spatial resolution and spectral quality through the use of spectro-ptychography at the Fe $L_3$ edge.

## INTRODUCTION

Magnetotactic bacteria (MTB) biomineralize membrane-enveloped, nano-sized magnetic crystals of magnetite ($Fe_3O_4$) or greigite ($Fe_3S_4$), known as magnetosomes [1]. Chains of magnetosomes are formed inside MTB. The net magnetic moment of the chain interacts with the Earth's geomagnetic field lines passively aligning the cell while the cell swims, a behavior called magnetotaxis. This, along with aerotaxis (chemotaxis to oxygen), is believed to help MTB locate and maintain position at the oxic-anoxic transition zone. MTB in the northern hemisphere swim preferentially towards geomagnetic north (North-seeking, NS), while those in the southern hemisphere swim towards geomagnetic south (South-seeking, SS) [1]. The difference between NS and SS behavior has been attributed to a reversed orientation of the magnetic moment of the magnetosome chain relative to the motile flagellum [2]. However, this hypothesis has never been verified experimentally.

For the past 6 years we have been developing X-ray magnetic circular dichroism (XMCD) measured in a soft X-ray scanning transmission X-ray microscope (STXM) as a tool to study the chemistry and magnetism of MTB on an individual cell and an individual magnetosome basis. Our proof-of-principle measurement was reported in 2011 [3], while an improved XMCD acquisition method and quantitative evaluation of the magnetic moment of the magnetite magnetosomes in a cultured marine MTB species, *Magnetovibrio blakemorei* strain MV-1, was reported in 2012 [4]. The ability to investigate the magnetism of each magnetosome in a cell, combined with an extensive study to build statistical precision, led to a realization that many MV-1 cells contain chains with gaps, and that, in a significant sub-set of such cells, the magnetism of the sub-chains on either side of the gap was opposed [5]. Since this reversal significantly reduced the net magnetic moment of those cells, we speculated as to the origin and possible evolutionary advantage of having such a 'defective' sub-population. One possibility was that such reversal cells might provide a mechanism to accommodate the periodic reversals of the earth's magnetic field. Another is that it provides a natural explanation for the frequent observation of a sub-population of oppositely directed cells in most MTB systems. Here we report an extension of that earlier study in which a connection is made to

*XRM 2014*
AIP Conf. Proc. 1696, 020002-1–020002-5; doi: 10.1063/1.4937496

proposed mechanisms of establishment of the single moment chain and how that moment is linked to the motile system in single-flagellum species such as MV-1, which are found in both the northern and southern hemispheres.

The spatial resolution of modern STXMs is typically 25-30 nm, which is only twice that of the typical 50 nm size of MV-1 magnetosomes. While we are able to measure XMCD of individual magnetosomes by over-sampling, improved spatial resolution and chemical specificity would greatly assist these and many other STXM studies. Recently soft X-ray spectro-ptychography [6,7] capabilities were developed at the Advanced Light Source (ALS). In addition to higher spatial resolution, ptychography improves chemical specificity due to reduced influence of the outer regions of the incident X-ray field [8]. Here we present our first results of applying ptychography to measure Fe $L_3$ spectra and XMCD of magnetosomes and MTB.

## EXPERIMENTAL

Cells of *Magnetovibrio blakemorei* strain MV-1 were grown anaerobically in liquid cultures with nitrous oxide as the terminal electron acceptor. Whole cell samples were prepared by pipetting a few μL of the culture onto a formvar-coated TEM grid, and subjecting the grid to 3 or 4 gentle wash cycles with increasingly dilute cell culture solution to remove salts without lysing the bacteria. Membrane-encased magnetite crystals were extracted from MV-1 by sonication, followed by magnetic separation and washing, using a procedure reported by Alphandéry *et al.* [9]. STXM measurements were made using ALS BL 5.3.2.2 (C 1s) and ALS BL 11.0.2 (Fe $L_3$). Ptychography measurements were performed on the new BL 11.0.2 microscope using a Princeton Instruments direct-sense X-ray camera (500 x 500 pixels), and a zone plate with 60 nm outer zone width and thus ~72 nm spot size. Ptychography diffraction patterns were measured at 50 nm spacing, giving ~40% overlap. It was important to regularly measure and correct for the background of the camera and stray light from the interferometer laser. With the Princeton Instruments camera both short (15 ms) and long (150 ms) signal acquisitions were made at each pixel. The short dwell time measurement recorded the bright field and low-q scattering signal without camera saturation while providing sampling of the diffraction signal to q=0. The long dwell time measurement provided the sensitivity needed to measure the diffraction signal at large q with good statistics. The combination of the short and long dwell time signals achieved the dynamic range required for high quality ptychographic imaging. The short and long dwell time signals were merged using the method described in the supplemental to ref. [7]. After correcting for the camera background, the array of ptychographic images was analyzed by a parallelized iterative approach, using the RAAR algorithm [10] implemented in the SHARP software [11], run on a multiple graphics processing unit (GPU) cluster computer. 500 iterations were used.

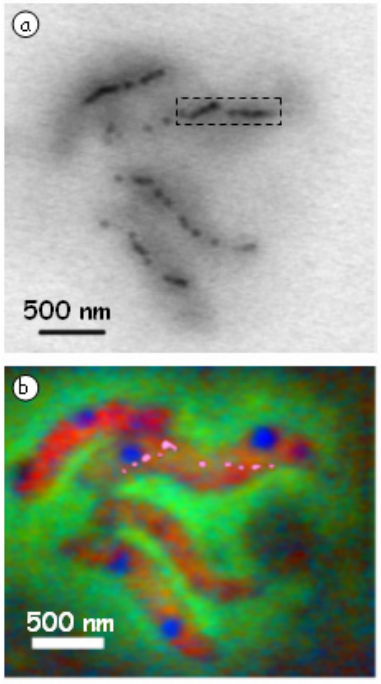


**FIGURE 1**. (a) Transmission STXM image at 710 eV of a set of 4 MV-1 cells, measured with a 25 nm zone plate. (b) Color coded composite of protein (red), extracellular polysaccharide (green) and lipid (blue) derived from a C 1s image sequence (280-310 eV). The pink objects are the ptychography signal of one cell at 710 eV measured in the region of the dotted rectangle in Fig. 1a.

## RESULTS AND DISCUSSION

**Figure 1** presents results from a conventional (25 nm outer zone width zone plate) STXM study of a sample of intact cells of *Magnetovibrio blakemorei* strain MV-1. **Figure 1a** shows the magnetosome chains

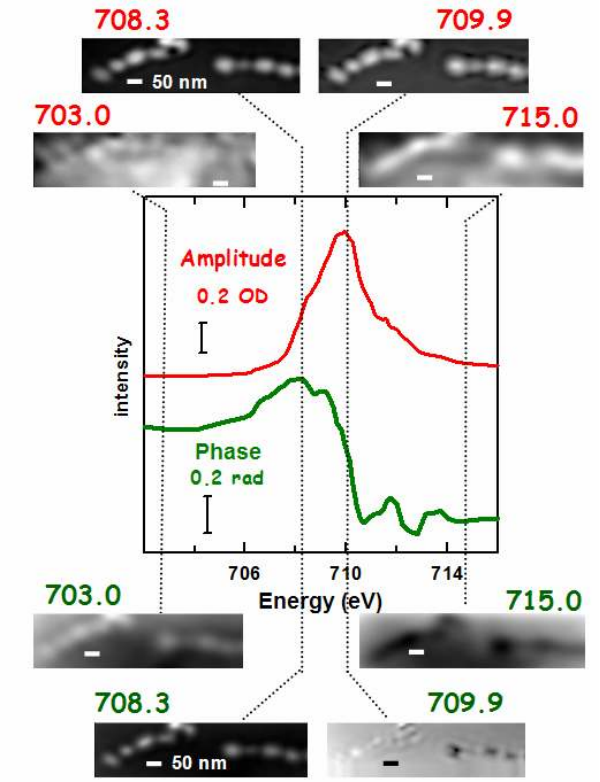


**FIGURE 2**. Amplitude (upper) and phase (lower) images and Fe $L_3$ spectra (using LCP) derived from a ptychographic image sequence consisting of 54 photon energies with a18 by 6 array of single pixel ptychography measurements at each energy. Each diffraction image (500 x 500 pixels) was measured using two dwell times (15 ms & 150 ms).

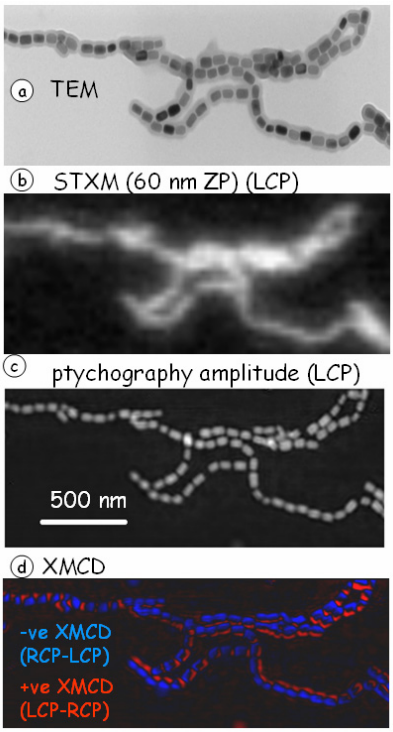


**FIGURE 3** (a) TEM ; b) STXM (60 nm ZP); (c) ptychography amplitude image (708.2 eV, left circular polarization - LCP), and (d) XMCD-ptychography signal recorded from chains of magnetosomes enclosed in a membrane extracted from MV-1 MTB (blue is positive and red is negative XMCD).

in each of four cells, with partial resolution of the individual magnetosomes. **Figure 1b** provides color coded maps of the biological components, with the cells being clearly visualized in the protein component map (red), the surrounding extracellular polysaccharide (EPS) in green, lipid-rich nodules in blue, and several other internal cellular features with a different character than the protein, polysaccharide or lipid rich regions, derived from the C 1s image sequence. The lipid-rich nodules were also observed by TEM and found to contain phosphorus [12]. The pink signal from the magnetosomes is that measured by ptychography at 710 eV.

**Figure 2** presents the Fe $L_3$ amplitude and phase spectra of the magnetosomes in a cell extracted from a spectro-ptychographic image sequence measured in the area of the dotted rectangle in Fig. 1a. Amplitude and phase images at four (of 54) photon energies are presented. As found in other spectro-ptychography studies [6-8], the contrast in the amplitude and phase signals is quite different. At present we are only using the amplitude signals but we expect a co-ordinated analysis of both phase and amplitude will yield further information, as has been demonstrated in the recent spectro-ptychographic study of Li $FePO_4$ battery materials [7].

**Figure 3** compares TEM (**Fig. 3a**), STXM (60 nm ZP, so reduced resolution, **Fig. 3b**), and ptychography images (**Fig. 3c**) of an array of magnetosome chains extracted from MV-1 MTB cells using a procedure which preserves the biological membrane in which the magnetosomes are grown. **Figure 3d** is the XMCD amplitude signal obtained by taking the difference of ptychography images measured at 708.2 eV (photon energy of the strongest XMCD signal of magnetite [3]) with left (LCP) and right (RCP) circular polarized light. The uneven contrast of different magnetosomes in the TEM image is caused by enhanced electron scattering at specific orientations, an effect which does not occur in the X-ray absorption (STXM) or ptychography signals.

**Figure 4** presents an analysis of the spatial resolution of the ptychography images using a simple 10-90% edge jump criteria. From these types of edge sharpness measurements over several of the magnetite crystals we estimate a spatial resolution of ~7 nm.

**Figure 5** compares Fe $L_3$ spectra of MV-1 magnetosomes measured using STXM with 2 different zone plates (25 nm and 60 nm) with the signal extracted from the ptychography amplitude images. Although the optical density should be similar in all 3 signals since the magnetosomes are all about the same thickness, the OD determined by ptychography is significantly stronger and most likely reflects the true optical density. The signals measured by STXM are weaker, because the X-ray probe has an extended spatial distribution and the contributions from the wings of the wavefront 'dilute' the absorption signal from the core of the magnetosome. As noted by Tyliszczak et al. [8], ptychography is better able than STXM to localize the true spectral signal, not just because of its higher spatial resolution, but also because the ptychographic reconstruction derives, and corrects for the wavefront shape. This is a general observation which points to significant benefits from ptychography in terms of spectroscopic and thus chemical sensitivity, in addition to the well documented enhancements of improved spatial resolution.

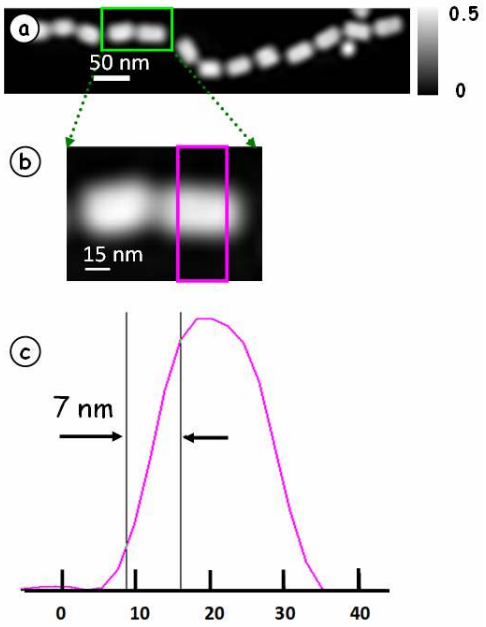


**FIGURE 4** (a) Sum of 25 ptychography amplitude images over the Fe $L_3$ edge, of a chain of extracted MV1 magnetosomes. (b) zoomed in image of two magnetosomes. (c) average vertical line profile across the indicated area.

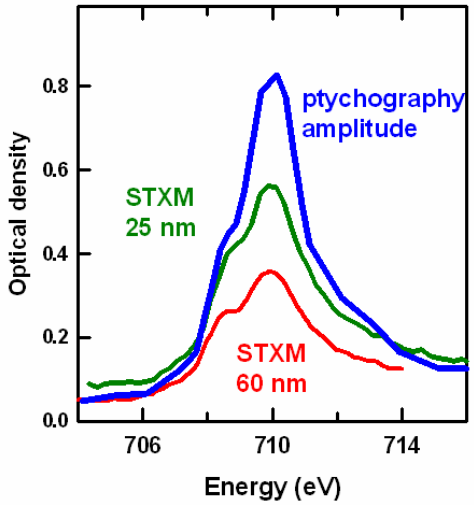


**FIGURE 5** Comparison of Fe $L_3$ spectra of MV-1 magnetosomes recorded with STXM using 25 nm and 60 nm outer-zone width zone plates, and with ptychography (60 nm ZP, 50 nm pixel spacing). In each case LCP was used.

While our studies are not yet complete, we have made measurements of the direction of the magnetic vector and presence or absence of gaps in the magnetosome chains from 18 South Seeking (SS) MV-1 cells from Rio de Janeiro, which complement our previous statistical study of North Seeking (NS) MV-1 cells [5]. In the SS sample there are many cells (10 of 18) which have chain gaps and a reversal of the magnetic vector on each side of the gap. In fact the proportion with gaps (56%) was significantly higher than that in the NS sample (19%) [5]. In addition, for the 8 SS cells with fully intact magnetosome chains (no gaps), 4 of them had an XMCD pattern indicating the magnetic vector was oriented with the vector pointing to the opposite end of the cell from the single flagellum, while the other 4 had the opposite orientation (magnetic vector pointing to the flagellum). A similar, ambiguous situation was also found for a recent study of chain orientation relative to flagellum in a population of NS cells. While additional measurements are needed to improve statistics, it seems that, relative to the flagellum, the orientation of the magnetic vector from magnetosome chains in NS and SS samples does not show the trend predicted by Torres de Araujo et al. [2]. We are exploring the hypothesis that the internally reversed chains arise from specifics of the chain formation mechanism, and give rise to a sub-population of cells with oppositely oriented magnetic vectors, relative to the cell flagellum. It is possible that a high rate of orientation error has an evolutionary advantage (e.g. for improving survival of magnetic pole reversal events, which have occurred every $2 \times 10^5$ years in the past 10-20 million years).

## SUMMARY

Spectro-ptychography at the Fe $L_3$ edge has been applied to studies of the magnetic properties of magnetosome chains from the magnetotactic bacterium *Magnetovibrio blakemorei* strain MV-1. Significant improvements in spatial resolution were demonstrated. Spatial resolutions in ptychographic imaging as low as 3 nm have been reported [7], but that was obtained at a much shorter wavelength. Our estimated 7 nm spatial resolution is the best so far for x-ray absorption imaging and spectroscopy around the Fe $L_{23}$ absorption edge. A large increase in spectro-ptychography spectral intensity was found relative to that observed in state-of-the-art STXM. Results for the orientation of magnetic moments relative to MV-1 flagella were reported and their significance with respect to biomineralization and magnetic orientation mechanisms briefly discussed.

## ACKNOWLEDGMENTS

Research funded by NSERC and Canada Research Chairs. Measurements were made at the Canadian Light Source (supported by NSERC, NRC, CIHR, and the U. Saskatchewan) and at the Advanced Light Source (supported by the Division of Basic Energy Sciences of U.S. DoE). This work is partially supported by the Center for Applied Mathematics for Energy Research Applications (CAMERA), which is a partnership between Basic Energy Sciences (BES) and Advanced Scientific Computing Research (ASRC) at the US Department of Energy. UL acknowledges support from Brazilian CNPq and FAPERJ. DAB is supported by US NSF grant EAR-1423939.

## REFERENCES

1. D.A. Bazylinski and R.B. Frankel, Nat. Rev. Microbiol. **2**, 217-230 (2004).
2. F.F. Torres de Araujo et al., Biophys J. **58**, 549-555 (1990).
3. S.S. Kalirai, K.P. Lam, D. Bazylinski, U. Lins and A.P. Hitchcock, Chemical Geology **300-301**, 14-23 (2012).
4. K.P. Lam, A.P. Hitchcock, M. Obst, J.R. Lawrence, G.D.W. Swerhone, G.G. Leppard, T. Tyliszczak, C. Karunakaran, J. Wang, K. Kaznatcheev, D. Bazylinski and U. Lins, Chemical Geology **270**, 110-116 (2010).
5. S.S. Kalirai, D.A. Bazylinski and A.P. Hitchcock, , Public Library of Science One **8,** e53368 (2013)
6. M. Beckers, T. Senkbeil, T. Gorniak, M. Reese, K. Giewekemeyer, S.-C. Gleber, T. Salditt, and A. Rosenhahn, Phys. Rev. Lett. **107**, 208101 (2011).
7. D.A. Shapiro, Y.-S. Yu, T. Tyliszczak, J. Cabana, R. Celestre, W. Chao, K. Kaznatcheev, A. L. D. Kilcoyne, F. Maia, S. Marchesini, Y. S. Meng, T. Warwick, L. L.Yang and H.A. Padmore, Nature Photonics **8,** 765-769 (2014).
8. T. Tyliszczak, H.-W. Shiu, W. Chueh, F. El Gabaly and D. Shapiro, "Soft X-Ray Spectromicroscopy Using Ptychography", poster S2-82, XRM2014, Melbourne, Au. 26-31 Oct 2014.
9. E. Alphandéry, Y. Ding, A. Ngo, Z. Wang, L. Wu and M. Pileni, ACS Nano **3,** 1539-1547 (2009)
10. D. R. Luke, Inverse Problems **21**, 37–50 (2005)
11. http://camera.lbl.gov/software/sharp_camera_downloads (accessed 20-Aug-2015)
12. F. Abreu, A.A. Sousa, M.A. Aronova, Y. Kim , D. Cox, R.D. Leapman, L.R. Andrade, B. Kachar, D.A. Bazylinski and U. Lins, J. Struc. Biol. **181,** 162–168 (2013).